International Journal of Fracture **44**: 111–131, 1990.

Determination of fracture energy, process zone length and brittleness number from size effect, with application to rock and concrete

Z.P. BAŽANT and M.T. KAZEMI
Center for Advanced Cement-Based Materials, Northwestern University, Evanston, Illinois 60208, USA

Received 20 August 1988; accepted in revised form 1 April 1989

Abstract. The dependence of the fracture energy and the effective process zone length on the specimen size as well as the crack extension from the notch is analyzed on the basis of Bažant's approximate size effect law. The fracture energy and the effective length of the fracture process zone is defined on the basis of the extrapolation to an infinite specimen size, for which the definitions are independent of the shape of the specimen or structure. Both of these material properties are expressed in terms of the size effect law parameters and the function describing the nondimensional energy release rate. Bažant's size effect law for the nominal stress σ_N at failure is reformulated in a manner in which the parameters are the fracture energy and the effective (elastically equivalent) process zone length. A method to determine these material properties from σ_N-data by linear and nonlinear regressions is shown. This method permits these properties to be evaluated solely on the basis of the measured maximum loads of specimens of various sizes and possibly also of different shapes. Variation of both the fracture energy and the effective process zone length as a function of the specimen size is determined. The theoretical results agree with previous fracture tests of rock as well as concrete and describe them adequately in relation to the inevitable random scatter of the tests.

1. Introduction

The fracture resistance of many heterogeneous aggregate materials such as rocks, concretes and various ceramics, as well as some metals, is increased by a toughening mechanism which is due to shielding of the crack tip by a nonlinear zone of distributed microcracking or void formation. In such materials the fracture energy requires a more careful definition and does not represent the sole material characteristic of fracture behavior. Another essential characteristic is the size of the nonlinear fracture process zone at the crack tip.

The size of the fracture process zone in which microcracking or void formation takes place is essentially, although not exclusively, a property of the material. It is determined by the size of the inhomogeneities in the microstructure, such as the maximum grain size in rock or the maximum aggregate size in concrete. If the size of this zone is negligible compared to the specimen or structure dimensions, the fracture behavior approaches that of linear elastic fracture mechanics. If the size of this zone encompasses all or most of the specimen or structure volume, the failure is determined by a strength or yield criterion. If the size of this zone is intermediate, the fracture behavior is transitional between the strength criterion and the linear elastic fracture mechanics. It is this transitional behavior which is of interest for many practical applications, and we focus on it in this study.

The nonlinear fracture process zone gives rise to a size effect which can be described by a rather simple size effect law recently proposed by Bažant [1–5]. It has been shown that this

law can be exploited to determine the fracture energy of the material merely by measuring the maximum loads of geometrically similar specimens of sufficiently different size [6–9].

The principal objective of this paper (whose principal results were summarized in recent conference preprints [10]) is to show that another basic material characteristic, namely the effective length of the fracture process zone, can also be extracted from the size effect data and that the size effect law can then be written in terms of the fracture energy and the effective process zone length, i.e., the material fracture parameters. The second objective is to demonstrate that the size effect law is applicable to fracture of various rocks. A new, simple formula for the R-curve from the size effect will also be presented.

2. Review of size effect law

The size effect in failure of geometrically similar specimens or structures of different sizes can be described in terms of the nominal stress at failure

$$\sigma_N = c_n \frac{P_u}{bd} \quad \text{for two-dimensional similarity,}$$
$$\sigma_N = c_n \frac{P_u}{d^2} \quad \text{for three-dimensional similarity,} \tag{1}$$

in which P_u is the maximum load (ultimate load), b = specimen thickness, d = characteristic dimension of the specimen (e.g., its length or depth) and $c_n = a$ coefficient introduced for convenience [2] (in some of the previous works of Bažant et al., coefficient c_n has been omitted and incorporated into the definition of d).

Note that if the specimens are geometrically similar, then all the formulas of stress analysis fall into the category of (1). For example, the elastic bending stress formula for a simply supported beam of depth d and span l may be written as $\sigma_N = 1.5P_u l/bd^2 = c_n P_u/bd$, which is equivalent to (1) with $c_n = 1.5l/d$ since l/d = constant if the specimens are geometrically similar. Likewise, if the nominal stress is defined by the plastic bending formula, one may write $\sigma_N = P_u l/bd^2 = c_n P_u/bd$ with $c_n = l/d$. The nominal stress for the beam could, of course, be defined by $\sigma_N = P_u/bl = c_n P_u/bd$ with $c_n = d/l$, or by various other formulas.

Making the hypotheses that the energy dissipated at failure is a smooth function of both the specimen (or structure) size and the fracture process zone width and that the latter is a constant, Bažant [4] showed by dimensional analysis and similitude arguments that

$$\sigma_N = Bf_u \{\beta[1 + \beta^{-1} + A_1\beta^{-2} + A_2\beta^{-3} + \ldots]\}^{-1/2}, \quad \beta = d/d_0, \tag{2}$$

in which B, d_0, A_1, A_2, . . . are empirical coefficients, f_u = some measure of tensile strength, and parameter β characterizes the relative structure size. Equation (2) represents an asymptotic expansion with respect to an infinitely large specimen. It was further demonstrated [9] that for the size range of up to about 1 : 20, the asymptotic series can be truncated after the

linear term. In that case (2) reduces to the size effect law proposed by Bažant [1, 2]:

$$\sigma_N = Bf_u\left(1 + \frac{d}{d_0}\right)^{-1/2}, \tag{3}$$

which we will exclusively use in this study; B and d_0 = empirical coefficients. For $d \gg d_0$, (3) yields $\sigma_N \propto d^{-1/2}$, which is the form of the size effect exhibited by every formula of linear elastic fracture mechanics. If $d \ll d_0$ then (3) reduces to $\sigma_N = Bf_u$, which is the value of the nominal stress at failure according to the strength (or yield) criterion. For the intermediate values of size d, (3) describes a gradual transition from the failures governed by the strength criterion (or the plastic yield criterion) to the failures governed by linear elastic fracture mechanics. Equation (3) was shown [9] to be valid not only for specimens which are similar in two dimensions but also for specimens similar in three dimensions (in which case σ_N is defined differently, see (1)).

The size effect law, (3), has the advantage that it can be transformed to a linear regression plot:

$$Y = AX + C, \tag{4}$$

in which

$$X = d, \quad Y = (f_u/\sigma_N)^2, \quad B = C^{-1/2}, \quad d_0 = C/A. \tag{5}$$

A represents the slope of the regression line of the measured σ_N-values in the plot of Y vs. d, and C is the Y-axis intercept of the regression line. In this manner coefficients B and d_0 can be easily determined from the measured values of the maximum load.

3. Verification of size effect law for rock

The applicability of (3) to concrete was amply verified for various specimen shapes by Bažant and Pfeiffer [8]. To verify this equation for rock, the test results of Hashida [11] and Hashida and Takahashi [12] for granite from the quarry at Iidate, Fukushima prefecture, Japan, have been analyzed. This rock is quite suitable for the present purpose since it is fairly coarse-grained with the average grain size 1.3 mm. The tests were made on the compact tension specimens shown in Fig. 1a, which were geometrically similar in two dimensions (except for negligible imperfections of the notch length); the thickness was varied; however, the influence of this should have been negligible.

The linear regression plot is shown in Fig. 2. It is apparent that as far as the statistical scatter of the results permits it to be seen, the results are in good agreement with the size effect law, (3). The regression analysis yields $A = 0.00173$/mm and $C = 0.172$, from which $d_0 = 99.4$ mm and $B = 2.414$. The coefficient of variation of the deviations of the data from the regression line is $\omega_{Y|X} = 0.128$. The coefficient of variation of the regression line slope is $\omega_A = 0.141$, and the correlation coefficient of the regression is $r = 0.971$. For the regression plot in Fig. 2, coefficient c_n was defined as $c_n = 2(2 + \alpha_0)/(1 - \alpha_0)^2$ in which $\alpha_0 = a_0/d$ where a_0 = the initial notch length. The modulus of elasticity of this rock was

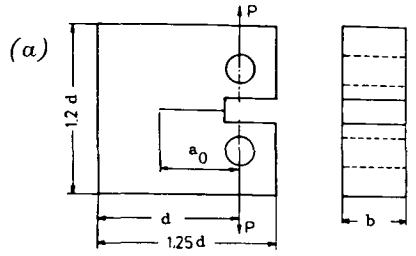

Specimen Label	b mm	d mm	a_0 mm	a_0/d	σ_N/f_u	$g(\alpha_0)$	$g'(\alpha_0)$
1TCT	20	58	31.7	0.553	2.063	132	915
2T	28	100	55.3	0.553	1.537	132	915
4T	50	200	107.0	0.539	1.425	120	804
6T	61	300	161.4	0.538	1.263	119	797
8T	77	400	214.8	0.537	1.050	118	789
Average				0.544			

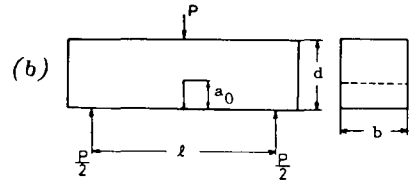

Specimen Label	b mm	ℓ mm	d mm	a_0 mm	a_0/d	σ_N/f_u	$g(\alpha_0)$	$g'(\alpha_0)$
1T Bend	30	80	30	9.5-15.8	-	2.59	-	-
2T	50	200	50	19.2,19.8	0.39	2.42	59	326
4T	104	271	105	37.5	0.357	1.68	18*	97*
20T	512	1356	508	207.0	0.407	1.28	26*	147*

*From Finite Element Method; other cases from Ref. [13].

Fig. 1. Geometries of the compact tension and three-point bend specimens used in Hashida and Takahashi's tests of granite.

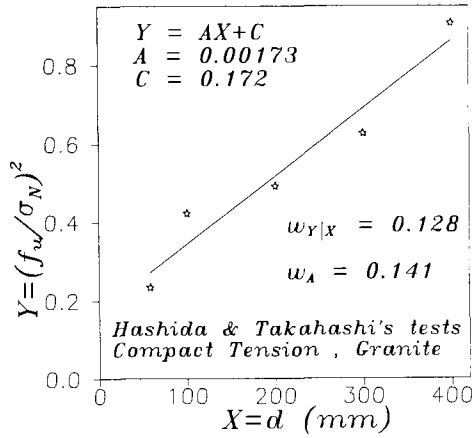

Fig. 2. Linear regression plot for granite, compact tension specimens with average $\alpha_0 = 0.544$.

measured to be $E = 29.4\,\text{GPa}$, and its direct tensile strength $f_u = 4.8\,\text{MPa}$, as obtained by uniaxial tension tests on cylindrical specimens of diameter 30 mm and length 50 mm.

The same authors have also made three-point bend tests with specimens of different sizes (Fig. 1b). For beams c_n was defined as $c_n = 3l/2d(1 - \alpha_0)^2$. These specimens, however, were not geometrically similar since they included different relative notch lengths and different span-depth ratios. The specimens other than the largest one were cut from the largest three-point bend specimen (512 × 508 × 1600 mm) after it had been tested.

1. Fracture energy from the size effect law

The total potential energy of a structure can always be written as $U = F(\alpha)\bar{U}V$, $V = bd^2$, $\bar{U} = (P/bd)^2/2E$ in which $\bar{U}$ = nominal strain energy density, V = nominal volume of the structure, and $F(\alpha)$ = certain function of the relative crack length, $\alpha = a/d$, where a = the crack length. The energy release rate, i.e., the energy released per unit thickness and unit extension of the crack length, may be calculated as $G = -(\partial U/\partial a)/b = -(\partial U/\partial\alpha)/bd$. This yields:

$$G = \frac{P^2}{Eb^2d}\,g(\alpha) \qquad (\alpha = a/d), \tag{6}$$

in which $g(\alpha) = -F'(\alpha)/2$ (the primes are used to denote derivatives), and load P is not necessarily the failure load P_u. All the formulas of linear elastic fracture mechanics have the form of (6). Equation (6) is valid for the conditions of plane stress. In the case of plane strain, E must be replaced by $E/(1 - \nu^2)$ where ν = Poisson's ratio. Function $g(\alpha)$ depends only on the specimen geometry, but not on its size. In linear elastic fracture mechanics it is shown that $G = K_I^2/E$ where K_I = mode I stress intensity factor. Thus, (6) is equivalent to

$$K_I = \frac{P}{b\sqrt{d}}\,f(\alpha), \tag{7}$$

in which $f(\alpha) = \sqrt{g(\alpha)}$. Again this is the typical form of all the formulas of linear elastic fracture mechanics. For many typical specimen geometries, the values of $f(\alpha)$ are listed in handbooks [13, 14]. Function $f(\alpha)$ or $g(\alpha)$ can also be obtained by linear elastic finite element analysis.

The crack propagates when K_I reaches the fracture toughness K_{Ic}, or G reaches the energy R required for further crack growth (in the J-integral method, $R = J_{Ic}$ = critical value of J_I); $R = K_{Ic}^2/E$.

As is well known, the values of R or K_{Ic} for materials with a large fracture process zone are highly size dependent if α in (6) or (7) is approximated as the relative initial notch or crack length, α_0. The J-integral method is somewhat less size-dependent but requires more measurements and more sophisticated instrumentation. The size dependence can be reduced by determining the actual crack length, a. However, this is not an easy task since the crack is not straight, does not run on a single line, and may extend discontinuously. Although various indirect methods, e.g., the compliance method, can estimate the crack length, a significant experimental error may occur for various reasons. Thus it seems attractive to

avoid the problem of determining the precise crack length altogether. This is made possible by the size effect method.

As proposed by Bažant [9], the fracture energy G_f may be uniquely defined as the energy required for crack growth in an infinitely large specimen. This value is, by definition, independent of test specimen size although this is true only approximately since the size effect law is not exact. G_f is also independent of the specimen shape. This becomes clear by realizing that in an infinitely large specimen the fracture process zone occupies a negligibly small fraction of the specimen's volume. Therefore, most of the specimen is elastic, which implies that the fracture process zone at its boundary is exposed to the asymptotic near-tip elastic stress and displacement fields which are known from linear elastic fracture mechanics and are the same for any specimen geometry. Here, the fracture process zone must be in the same state regardless of the specimen shape.

For the size effect law to apply to similar notched specimens, the maximum load must be reached before the fracture process zone detaches itself from the notch tip. This is guaranteed only if we restrict consideration to those specimens for which $g'(\alpha_0) > 0$. Such behavior, which precludes stable crack growth, according to linear elastic fracture mechanics, is true for most geometries (exceptions are e.g., the double cantilever specimen, center-cracked specimen loaded on the crack, chevron notch specimen, and slanted compact tension specimen). Then, considering the limit $d \to \infty$, one should also note that $\alpha \to \alpha_0 = a_0/d$ (a_0 = notch length or initial crack length) because the size of the fracture process zone must remain of the same order of magnitude as the material inhomogeneities. If we substitute P_u according to the size effect law (3) into (6), we obtain

$$G_f = \lim_{d\to\infty} R = \lim_{d\to\infty} \frac{P_u^2 g(\alpha)}{Eb^2 d} = \frac{B^2 f_u^2}{c_n^2 E} \lim_{d\to\infty} \frac{d}{1 + d/d_0} \lim_{\alpha\to\alpha_0} g(\alpha), \tag{8}$$

which yields

$$G_f = \frac{B^2}{c_n^2 E} f_u^2 d_0 g(\alpha) = \frac{f_u^2}{c_n^2 AE} g(\alpha_0). \tag{9}$$

The last expression uses directly the slope of the size effect regression line [9].

Using (9) with $\alpha_0 = 0.544$, one obtains from the test results of Hashida and Takahashi for Iidate granite the value $G_f = 94\,\mathrm{J\,m^{-2}}$. Hashida measured the critical J-integral value by the acoustic emission method on his compact tension and three-point-bend specimens. He concluded that, for this method, J_{1c} is size independent and has the value $J_{1c} = 107\,\mathrm{J\,m^{-2}}$.

Abe, Hayashi and Hashida [15] also determined J_{1c} by analyzing the results of some hydraulic fracturing experiments on very large specimens of the same rock (10.4 m × 9.3 m × 8.8 m). The test results were analyzed by the modified boundary element method in which the crack was assumed to expand as a semi-elliptical crack such that its K_1 is constant along its periphery. It was found that the fracture toughness of this granite is independent of the crack size and is $1.93\,\mathrm{MPa\,m^{1/2}}$. This corresponds to $R = 126\,\mathrm{J\,m^{-2}}$. The differences among the aforementioned values are within the range of the experimental scatter that one must expect. Among the experimental methods used, the size effect method is the simplest.

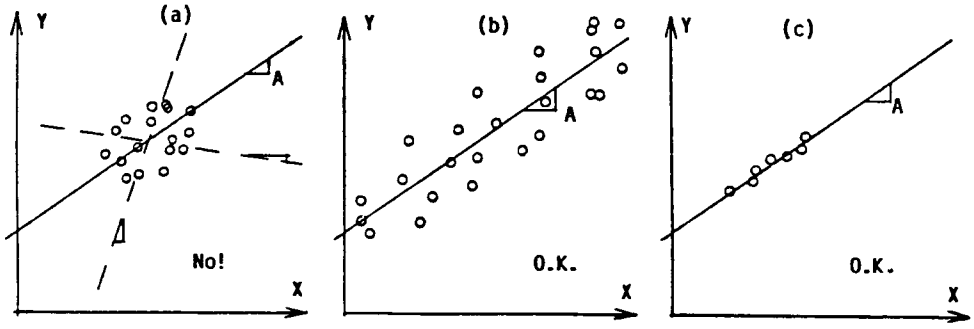

Fig. 3. (a) Size-effect method is inapplicable when the size range is too small compared to scatter; (b, c) size range is sufficient.

The necessary range of sizes depends on the scatter produced by random variability of material properties and experimental errors. The larger the scatter, the broader is the range required. For the usual scatter obtained for rock or concrete, it seems that the size range of 1 : 4 is sufficient to obtain the mean values of material parameters, and the range of at least 1 : 8 is required to verify the applicability of the size effect law. When the range is insufficient for the scatter experienced, the results may be meaningless, as illustrated in Fig. 3 taken from Bažant and Pfeiffer [8].

Because the size effect law in (3) is only approximate, applicable to a size range up to about 1 : 20, the definition of G_f as the energy required for infinitely large specimens should not be interpreted literally. In practice, the infinite size means merely a size which is just beyond the range of applicability of the size effect law for which this law has been calibrated. This seems good enough for most practical purposes. However, for structure sizes that are orders of magnitude larger than the end of the size range used in calibration, the values of the fracture energy can be substantially different, and it would be necessary to take more terms in the expansion in (2) or use for the size effect some other type of formula with more parameters.

5. Elastically equivalent crack length

The elastic stress and displacement fields surrounding the nonlinear fracture process zone correspond to a certain effective (or elastically equivalent) crack length a. Let $\alpha = a/d$ = relative crack length. For the maximum load, one may write

$$a = a_0 + c, \quad \alpha = \alpha_0 + c/d, \tag{10}$$

in which a_0 is the initial length of the notch or the crack, and $\alpha_0 = a_0/d$. Supposing that for the corresponding linear elastic problem with crack length a the fracture growth under constant loads is unstable, c represents the equivalent length of the nonlinear fracture process zone. Obviously the value of c must be bounded as $d \to \infty$. This limit value, denoted as c_f, must represent a property of the material, since in an infinitely large specimen the boundary geometry can have no effect on the elastic field surrounding the nonlinear fracture process zone. Therefore, the limit effective length of the nonlinear fracture process zone must

be a constant material property if it is defined as

$$c_f = \lim_{d\to\infty} (a - a_0). \tag{11}$$

According to (9) and (6) with $P = P_u$ calculated from (3), we obtain

$$G_f - G = \frac{f_u^2}{c_n^2 EA}\left[g(\alpha_0) - \frac{d}{d_0 + d}\, g(\alpha)\right]. \tag{12}$$

Since we must have $G \to G_f$ when $d \to \infty$, it follows that

$$g(\alpha_0)\,(d + d_0) = g(\alpha)d. \tag{13}$$

Function $g(\alpha)$ is continuous and smooth, and for α close to α_0 it may be approximated as

$$g(\alpha) = g(\alpha_0) + g'(\alpha_0)\,(\alpha - \alpha_0) = g(\alpha_0) + g'(\alpha_0)\,\frac{c_f}{d}, \tag{14}$$

in which (10) for $c \to c_f$ has been used. Substitution of (14) into (13) finally yields the following expression for the effective (elastically equivalent) fracture process zone length:

$$c_f = \frac{g(\alpha_0)}{g'(\alpha_0)}\, d_0. \tag{15}$$

It should be pointed out that the value of c_f is more sensitive to experimental or numerical error than G_f. The reason is that c_f depends not only on $g(\alpha_0)$ but also on the derivative $g'(\alpha_0)$ (15) while G_f depends only on $g(\alpha_0)$. The derivatives have larger errors than the values of functions. The value of G_f is determined primarily by equilibrium conditions, while the values of $g'(\alpha_0)$, and thus also c_f, is related to stability considerations [16].

The value of c_f determined in this manner must also be independent of the specimen shape. The reason is the same as already explained for G_f.

From the test results of Hashida and Takahashi on the compact tension specimens of Iidate granite, (15) yields $c_f = 14.6\,\text{mm} = 0.15 d_0$, on the basis of the values obtained by the size effect linear regression. This value is about 11-times the grain size d_g for this rock.

Nonlinear optimization of the fits of the maximum load data for these tests based directly on (3) (with $\alpha_0 = 0.544$ as the average value) yields slightly different values: $G_f = 88\,\text{J m}^{-2}$, and $c_f = 12.1\,\text{mm}$. The reason for this difference is, of course, the fact that the objective function differs from that implied in the linear regression analysis in the transformed variables Y and X.

6. Size effect law with parameters independent of specimen shape

By inversion of (15) we have

$$d_0 = \frac{g'(\alpha_0)}{g(\alpha_0)}\, c_f. \tag{16}$$

Furthermore, from (5), $B = C^{-1/2} = (d_0 A)^{-1/2}$, and substitution of A calculated from (9) provides

$$B = \frac{c_n}{f_u}\left(\frac{EG_f}{c_f g'(\alpha_0)}\right)^{1/2}. \tag{17}$$

Introducing these values into (3), we obtain

$$\sigma_N = c_n\left(\frac{EG_f}{g'(\alpha_0)c_f + g(\alpha_0)d}\right)^{1/2}. \tag{18}$$

In this form of the size effect law of Bažant the parameters are true material parameters, G_f and c_f. The effect of structure shape is introduced solely by $g(\alpha_0)$ and $g'(\alpha_0)$. Note that (18) can also be written as $\sigma_N = c_n(EG/g(\alpha)d)^{1/2}$, but this expression can be used only after α and G are determined (which will be discussed later in connection with the R-curve).

In specimens with more than one crack tip, two or more crack tips could be in a critical state simultaneously. Then either a single crack tip can propagate, or more than one crack tip can propagate. For example, in the double-edge-notched bar under symmetric tension, either both cracks can propagate symmetrically, which we call the main path, or only one crack may propagate asymmetrically, which we call the secondary path. Experiments indicate preference for the secondary path; for rock see, e.g., Labuz, Shah and Dowding [17]. The path which actually occurs after path bifurcation can be determined on the basis of (18), in which the values of $g(\alpha_0)$ are the same for both paths but the values of $g'(\alpha_0)$ are different. From the condition that the internal entropy increment of the specimen must be maximum among all the paths, it has been shown [18] that the actual path (called the stable path) is that for which the curve $P(u)$ or $\sigma(u)$ has the mildest ascent (u = load-point displacement). It follows that the peak value σ_N which actually occurs must be the lowest among all the paths, and according to (18) this happens if $g'(\alpha_0)$ is the largest. For our double-edge-notched tension specimen with $\alpha_0 = 1/6$ one obtains $g'(\alpha_0) = 4.1$ and 6.3 for the symmetric and asymmetric crack propagations. This means that one crack will propagate asymmetrically from one side, with $g'(\alpha_0) = 6.3$.

Note that (18) also implies the bifurcation to occur before the peak load, except when $c_f/d \to 0$, in which case the bifurcation occurs at the peak load (this is the case of linear elastic fracture mechanics).

Equation (3) can be used only for specimens of the same shape, because parameters B and d_0 depend on the geometry of the specimen. Equation (18), by contrast, has the advantage that it applies to specimens of all sizes and all shapes. Therefore, it can be used for a collective nonlinear regression analysis of a large set of data from specimens of different sizes which are not geometrically similar, and possibly have very different shapes. Such nonlinear regression can be carried out by nonlinear optimization subroutines such as that of Levenberg and Marquardt. However, the optimization results based on (18) would be biased due to the fact that the definitions of d and σ_N are arbitrary. To overcome this problem, (18) may be rewritten as

$$\tau_N = \left(\frac{EG_f}{c_f + D}\right)^{1/2}, \quad \text{with } \tau_N = \frac{\sqrt{g'(\alpha_0)}}{c_n}\sigma_N = \sqrt{g'(\alpha_0)}\,\frac{P_u}{bd}, \quad D = \frac{g(\alpha_0)}{g'(\alpha_0)}d, \tag{19}$$

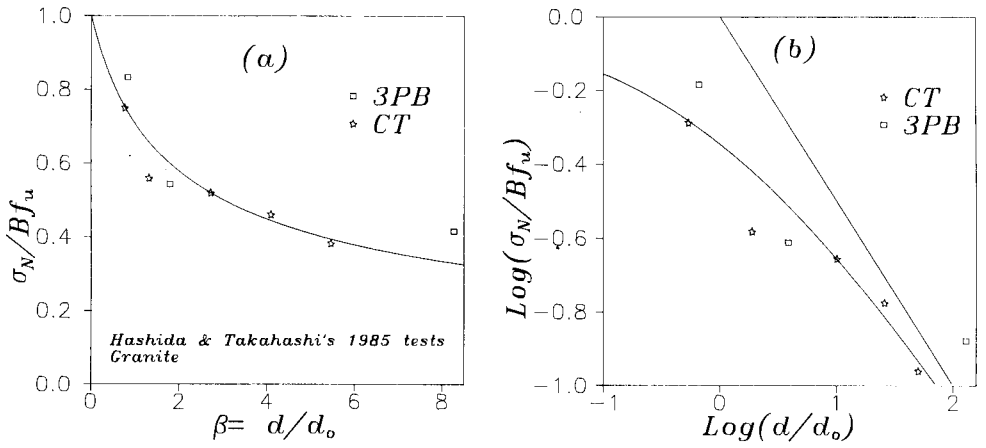

Fig. 4. Size effect plot obtained by collective fitting of granite test results (CT = compact tension specimen, 3PB = three-point-bend specimen).

in which τ_N and D represent the shape-independent nominal strength and the shape-independent characteristic dimension of the specimen. Here $\alpha_0 = a_0/d$ must of course be based on the same d as σ_N (1).

For the compact tension specimens of Hashida and Takahashi (Fig. 1a), nonlinear optimization of the fit of the test data with (19) yields $G_f = 91\,\mathrm{J\,m^{-2}}$ and $c_f = 13.3\,\mathrm{mm}$. From the data for the largest three specimen sizes of the three-point bend specimens (Fig. 1b), the nonlinear optimization yields $G_f = 97\,\mathrm{J\,m^{-2}}$ and $c_f = 9.4\,\mathrm{mm}$. Furthermore, a collective nonlinear optimization of the fit of the test results for both the compact tension and three-point bend specimens of Hashida and Takahashi yields $G_f = 91\,\mathrm{J\,m^{-2}}$ and $c_f = 11.0\,\mathrm{mm}$. The size effect relation obtained by this collective analysis of all the test data is plotted in Fig. 4.

Equation (19), just like (3), has also the advantage that it can be algebraically transformed to a linear regression equation:

$$Y^* = A^*X^* + C^*, \tag{20}$$

in which

$$Y^* = \frac{1}{\tau_N^2} = \frac{c_n^2}{g'(\alpha_0)\sigma_N^2}, \quad X^* = D = \frac{g(\alpha_0)}{g'(\alpha_0)}\,d, \quad EG_f = \frac{1}{A^*}, \quad c_f = \frac{C^*}{A^*}. \tag{21}$$

Here A^* represents the slope of the regression line.

The linear regression according to (20)–(21) gives slightly different results from the nonlinear optimization of the data fits according to (19). The reason is that each type of optimization implies a different weighting of the errors since it minimizes a different objective function. For Hashida and Takahashi's data on Iidate granite, the results are summarized in Table 1. The linear regression of compact tension test results yields $G_f = 97\,\mathrm{J\,m^{-2}}$ and $c_f = 15.8\,\mathrm{mm}$; the coefficient of variation of the deviations of Y^* from the regression line is $\omega_{Y^*|X^*} = (s_{Y^*|X^*})/\bar{Y}^* = 13.1\%$, where $\bar{Y}^*$ = mean of the experimental Y^*-values

Table 1. Results from Hashida and Takahashi's (1985) Data for Rock (CT = compact tension specimen, 3PB = three-point-bend specimen)

Specimen Type	By linear regression			By nonlinear regression		
	G_f J m $^{-2}$	c_f mm	ω %	G_f J m^{-2}	c_f mm	ω %
CT (average $\alpha_0 = 0.544$)	94	14.6	9.16	88	12.1	8.92
CT (different α_0)	97	15.8	9.48	91	13.3	9.26
3PB	180	36.8	27.60	97	9.4	20.65
CT & 3PB (combined)	148	34.3	17.10	91	11.0	12.56

For the three-point-bend tests only three data points were available. The linear regression results obtained for the three-point-bend tests separately and with the compact tension tests collectively are not as accurate as nonlinear analysis. In Table 1, ω = coefficient of variation of the deviations of the test results from (19). For all the cases, the value of ω obtained from the nonlinear analysis is less, because the objective function in that case is the sum of the squares of the deviations in τ_N.

Experimental data on the size effect that are more extensive than those which exist for rock have been obtained by Bažant and Pfeiffer [8] for concrete and mortar–rock-like materials. These data also included very different specimen shapes, in particular three-point-bend specimens (with $g(\alpha_0) = 6.07$, $g'(\alpha_0) = 35.2$), eccentric compression double-edge-notched specimens (with $g(\alpha_0) = 1.47$, $g'(\alpha_0) = 6.57$) and edge-notched tension specimens (with $g(\alpha_0) = 0.593$, $g'(\alpha_0) = 6.32$; the latter value corresponds to assuming that only one of the two cracks propagates, breaking symmetry). These specimens model the case of a pure tensile force loading, a pure bending moment loading, and a combined compression force-moment loading of the ligament section. This covers the entire range of loadings which can be obtained for different specimen shapes.

For the same actual specimen dimension, the case of pure tensile loading is the farthest from the linear elastic fracture mechanics because the fracture process zone is as large as the ligament size; the shape-independent dimensions D range from 3.5 mm to 14.0 mm. The case of compression loading, for which D = 8.4 mm to 67.2 mm, is the closest to the linear elastic fracture mechanics, because the compression loading forces the fracture process zone to be small relative to the ligament size. The case of bending, for which D ranges 6.5 mm to 52.0 mm, is intermediate. Figure 5 shows linear regression of these data. Despite these differences, the size effect tests on all the three types of specimens yielded nearly the same value of the fracture energy, and thus verified the applicability of the size effect method.

Although the aforementioned experimental study was extensive, it did not include data analysis on the basis of (19)–(21). The linear and nonlinear optimization of Bažant and Pfeiffer's test results according to (19)–(21), made for all specimens sizes and all specimen shapes, are summarized in Table 2. As it is seen from Table 2, the results for c_f from different types of specimens are not very different for concrete. But for mortar, the value of c_f for the notched tension specimens is much larger than for the other specimens. It must be pointed out, though, that the size range of the notched tension specimens tested was less than for the other specimens (1 : 4 compared to 1 : 8), and the data points were all located on the curved part of the size effect curve, far away from the straight-line asymptote for large sizes. This must have caused a large random error in the results for the notched tension specimens. Moreover, the collective optimization, consequently, implies a larger weight for the data

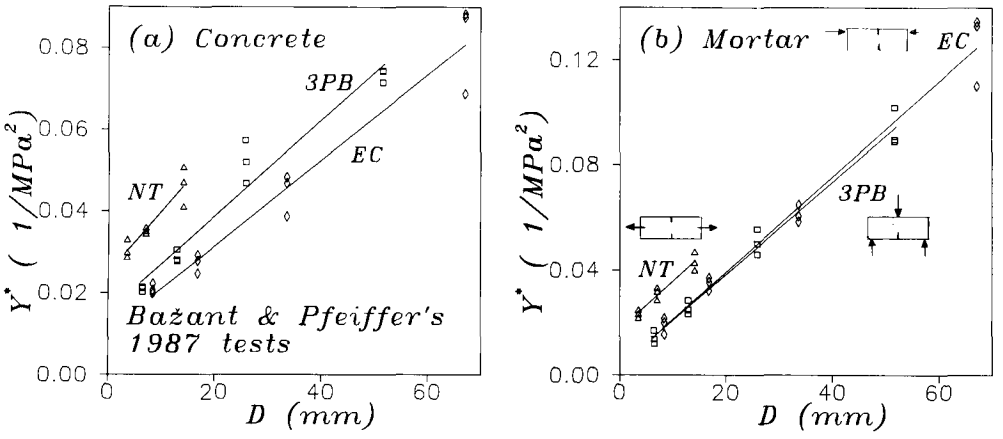

Fig. 5. Linear regression plots for concrete and mortar (NT = notched tension specimens, 3PB = three-point-bend specimens, EC = eccentric compression specimen).

Table 2. Results from Bažant and Pfeiffer's (1987) Data for Concrete and Mortar (NT = notched tension specimen, EC = eccentric compression specimen)

Specimen type	By linear regression			By nonlinear regression			E (mean) GPa
	G_f J m $^{-2}$	c_f mm	ω %	G_f J m^{-2}	c_f mm	ω %	
a. Concrete							
3PB	37	13.5	5.56	32	9.4	4.04	27.6
NT	31	16.8	3.42	32	17.4	3.41	25.5
EC	39	10.3	5.21	43	13.2	4.68	29.0
3PB & EC	39	13.7	6.81	38	12.2	6.56	28.3
3PB & EC & NT	47	23.6	12.82	51	25.7	12.66	27.4
b. Mortar							
3PB	20	1.9	7.11	20	1.2	6.73	32.9
NT	20	9.3	3.67	19	8.7	3.62	32.2
EC	20	1.8	6.60	20	2.2	6.54	32.8
3PB & EC	20	1.7	6.63	20	1.3	6.58	32.9
3PB & EC & NT	22	6.4	16.30	27	9.6	15.81	32.7

points in the curved part of the size effect plot, thereby making c_f and G_f larger for these specimens. Aside from that, the competition of the symmetric and asymmetric propagation modes might be an additional error-producing factor for the double-edge-notched tension specimens.

Due to the fact that there are two crack tips, the crack propagation path bifurcates. The stable path is that for which only one crack grows asymmetrically. This causes the value of $g'(\alpha_0)$ to be higher than that used in Bažant and Pfeiffer's work [8]. In that work, however, only G_f was analyzed, and it so happens that, unlike c_f, the value of G_f does not depend on $g'(\alpha_0)$.

It may be noted that the bifurcation point marking the onset of nonsymmetry is size-dependent in the case of R-curve behavior. However, due to the finite size of the fracture process zone, the bifurcation is not sharply delimited but crack propagation should change from symmetric to single crack gradually. This behavior may produce additional uncertainty in the equivalent value of $g'(\alpha_0)$ and make it size dependent.

7. Brittleness number

To characterize the brittleness of the structural response quantitatively, various definitions of the so-called brittleness numbers have recently been proposed by Hillerborg [19], Carpinteri [20] and Bažant [9]. Only Bažant's brittleness number β, however, is independent of the geometrical shape of the specimen, which was justified experimentally in Bažant and Pfeiffer [8]. This brittleness number is defined as $\beta = d/d_0$ and according to (15) and (19) its value may be calculated as

$$\beta = \frac{g(\alpha_0)}{g'(\alpha_0)} \frac{d}{c_f} = \frac{D}{c_f}, \tag{22}$$

in which $D = dg(\alpha_0)/g'(\alpha_0)$ = effective structural dimension. The functions of α_0 represent the necessary correction of the ratio d/c_f which makes β independent of the geometrical shape.

When $\beta > 10$, the failure may be analyzed according to linear elastic fracture mechanics. When $\beta < 0.1$, the failure may be analyzed on the basis of the strength criterion or plastic limit analysis. For $0.1 < \beta < 10$, nonlinear fracture analysis is required. The size effect law in (3) or (18) makes it nevertheless possible to calculate the failure load within nonlinear range on the basis of linear elastic fracture mechanics, provided the values of G_f and c_f are known. This greatly simplifies practical applications.

Since various types of brittle failures of concrete structures, such as the diagonal shear of beams, punching shear of slabs, torsion of beams, pull-out of bars, and beam and ring failures of pipes are within the range of nonlinear fracture mechanics and have been shown to follow Bažant's size effect law, the use of the brittleness number can considerably simplify failure calculations.

8. *R*-curves from size effect

For a fixed specimen geometry, and approximately also for a narrow range of similar geometries, the dependence of the energy R required for crack growth on the crack extension c from the notch can be considered to be a material property, called the R-curve, as proposed by Irwin [21] and Krafft [22]. The usual methods of measurement of the R-curve rely on some direct or indirect determination of the crack length. Recently, it has been shown by Bažant, Kim and Pfeiffer [6] that the R-curve can be easily determined from the size effect. We now analyze this subject in greater depth, focusing not only on the variation of R but also on the variation of the effective length of the fracture process zone.

Consider the energy W (under isothermal conditions the Helmholtz free energy), which must be supplied to deform the body and produce a crack of length $c = a - a_0$; $W = U + b \int R(c)\, dc$. Fracture propagation at no change in loads is possible when $\delta W/b = -G\delta a + R\delta c = 0$, in which $G = -(\partial U/\partial a)/b = G(\alpha, d)$. From this, the necessary condition for fracture propagation is $G - R = 0$, i.e.,

$$R(c) = G(\alpha, d), \tag{23}$$

in which $\alpha = \alpha_0 + c/d$. Failure occurs if fracture propagation is possible also for the next adjacent state, which means that $\partial F(c, d)/\partial d = 0$ where $F(c, d) = G - R$, because a change in d implies a change in the crack length if α_0 is fixed. Since $\partial R(c)/\partial d = 0$, we obtain for the failure states at various d the condition

$$\partial G(\alpha, d)/\partial d = 0. \tag{24}$$

Geometrically, (23)–(24) mean that the curve $R(c)$ is the envelope of the curves $G(\alpha, d)$ for all specimen sizes d. This property was exploited for determining the R-curve by Bažant, Kim and Pfeiffer [6].

Although the construction of the R-curve as an envelope is instructive, it would be easier to have an explicit formula. Such a formula can be derived, as we now show. We have $P_u^2 = (\sigma_N bd/c_n)^2 = (Bf_u bd/c_n)^2(1 + d/d_0)$ where $(Bf_u)^2 = c_n^2 EG_f/d_0 g(d_0)$, according to (9). If we substitute this into $G = P_u^2 g(\alpha)/Eb^2 d$ (6), we obtain for the critical states at maximum loads

$$G(\alpha, d) = R(c) = G_f \frac{g(\alpha)}{g(\alpha_0)} \frac{d}{d + d_0}. \tag{25}$$

Substituting this into (24), differentiating and noting that $\partial\alpha/\partial d = \partial\alpha_0/\partial d + \partial(c/d)/\partial d = -c/d^2 = -(\alpha - \alpha_0)/d$ (because α_0 = constant or $\partial\alpha_0/\partial d = 0$ for geometrically similar structures), we get

$$d + d_0 = \frac{g(\alpha)d_0}{(\alpha - \alpha_0)g'(\alpha)}. \tag{26}$$

Substituting this, along with the relations $(\alpha - \alpha_0)d = c$ and $d_0 = c_f g'(\alpha_0)/g(\alpha_0)$ (from (16)), into (25), we obtain the following basic result:

$$R(c) = G_f \frac{g'(\alpha)}{g'(\alpha_0)} \frac{c}{c_f}, \tag{27}$$

where c_f represents the value of c as $d \to \infty$ (15). Furthermore, substituting this into (25), we obtain the dependence of the effective length c of the fracture process zone at maximum load on size d:

$$c = c_f \frac{d}{d + d_0} \frac{g'(\alpha_0)}{g'(\alpha)} \frac{g(\alpha)}{g(\alpha_0)}. \tag{28}$$

To get further insight into the shape of the R-curve corresponding to the size effect law, we may obtain from (27), (16), and (26) the following relations:

$$\left[\frac{\partial R}{\partial c}\right]_{c=0} = \frac{G_f}{c_f} \frac{g'(\alpha_m)}{g'(\alpha_0)}, \tag{29}$$

$$\left[\frac{\partial R}{\partial c}\right]_{c=c_f} = 0. \tag{30}$$

Here α_m is a limiting value of α as $d \to 0$. From (26) we find that

$$\alpha_m = \alpha_0 + \frac{g(\alpha_m)}{g'(\alpha_m)}, \tag{31}$$

which represents an implicit algebraic equation for α_m (the maximum value of α).

The value of the fracture energy required for further crack growth can also be evaluated as $R = G$ from (26) and (6). Based on the experimental maximum load value P_t obtained in tests, the corresponding R-value is:

$$R_t = \frac{P_t^2}{Eb^2 d} g(\alpha). \tag{32}$$

Equations (27) and (26) define the R-curve corresponding to the size effect law parametrically. To construct the R-curve, we must first determine G_f and d_0 on the basis of the size effect law. Then we choose a series of α-values. For each of them we evaluate d, get

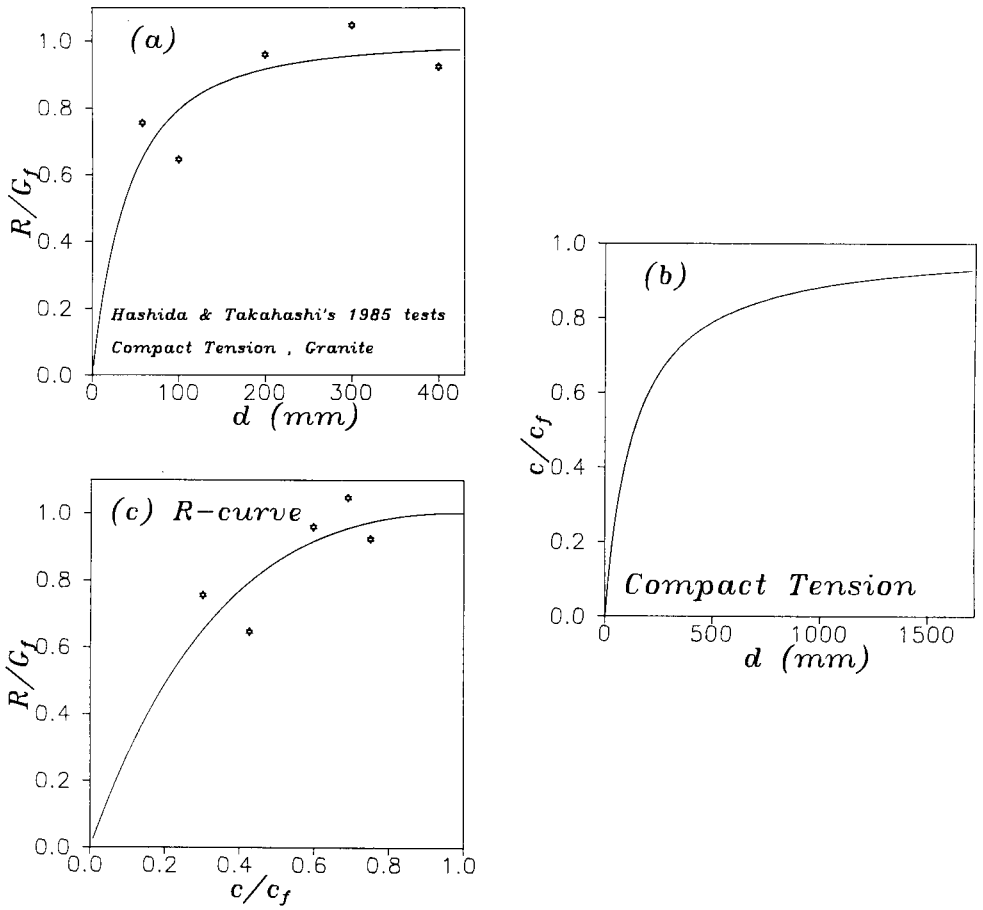

Fig. 6. Dependence of R and c on size and R-curve for compact tension specimen (average $\alpha_0 = 0.544$).

$c = (\alpha - \alpha_0)d$, and calculate R from (27). (The values of d in this calculation represent specimen sizes for which the maximum load occurs at crack length c.) If c is given, the corresponding value of R must be solved from (26)–(27) by Newton iterations. The dependence of the fracture toughness required for crack growth on c and d can be obtained from the relation $K_{Ic} = (ER)^{1/2}$.

The foregoing derivation of the R-curve presumed the fracture process zone to remain attached to the tip of the notch or initial crack. This ceases to be true after the peak load. The fracture process zone becomes detached from the tip and thus its size should remain approximately constant. Consequently, it should dissipate roughly the same amount of energy per unit crack extension. Accordingly, the value of G after the peak load must be kept in calculations constant and equal to the value that $R(c)$ attained at the peak load (experimental evidence to this effect is presented in [7]). So, the asymptotic value G_f of the R-curve can be reached only if the specimen size tends to infinity.

For the compact tension tests of Hashida and Takahashi with $\alpha_0 = 0.544$, one obtains $\alpha_m = 0.653$. This means that for extremely small specimens the effective fracture process zone length would represent 20 percent of the ligament cross section. Figure 6(a, c) shows the scatter of the R_i values obtained from the maximum loads and the smoothed curves of

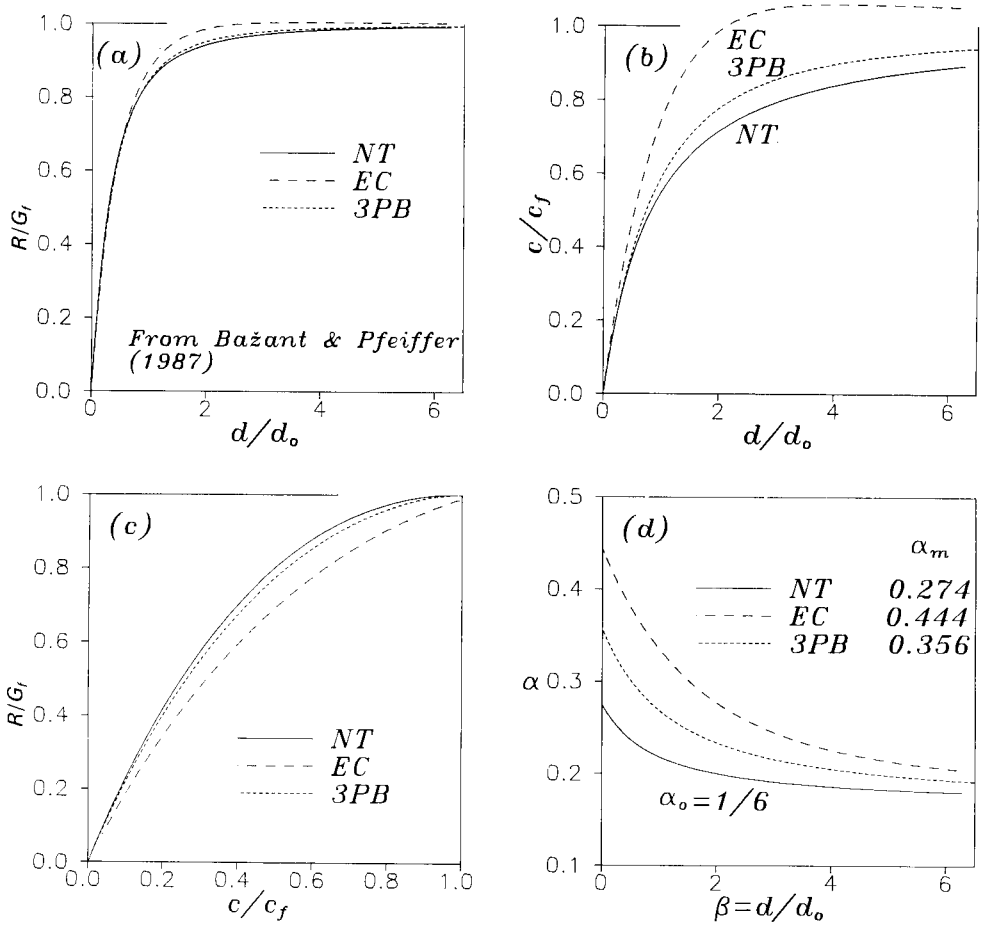

Fig. 7. Dependence of R, c and α on size and R-curve for Bažant and Pfeiffer's specimens.

R as a function of d and c, obtained from the size effect law. Figure 6b shows the variation of c as a function of d. It should be noted that the values calculated directly from the experiments are very scattered. Clearly some theory, such as Bažant's size effect law, is necessary to smooth out the results.

Figures 7c and 7(a, b) show the R-curve and the variations of the fracture energy and process zone length which were calculated for specimens used by Bažant and Pfeiffer [8] (NT = notched tension, 3PB = three-point-bend, and EC = eccentric compression specimens). Figure 7d shows the relative total crack length, α, as a function of d for different specimens.

9. Simplified variation of R and fracture process zone length

If the specimen is relatively large, the fracture process zone length may be neglected, i.e., one may set $\alpha = \alpha_0$. Then, (6) yields the approximation

$$R = \frac{P_u^2}{Eb^2 d} g(\alpha_0). \tag{33}$$

Substituting for P_u the value for the size effect law, (1) and (3), and expressing f_u' by means of the fracture energy, (9), one obtains

$$\frac{R}{G_f} = \frac{d}{d + d_0} = \frac{\beta}{1 + \beta}. \tag{34}$$

Figure 8 shows the test results of Hashida and Takahashi fitted by (34).

Using the relations $K_{Ic} = (ER)^{1/2}$ and $K_{Icf} = (EG_f)^{1/2}$, one obtains from (34) the approximate variation of the apparent fracture toughness with the specimen size:

$$\frac{K_{Ic}}{K_{Icf}} = \left(\frac{d}{d + d_0}\right)^{1/2} = \left(\frac{\beta}{1 + \beta}\right)^{1/2} \tag{35}$$

given by Bažant and Pfeiffer [8].

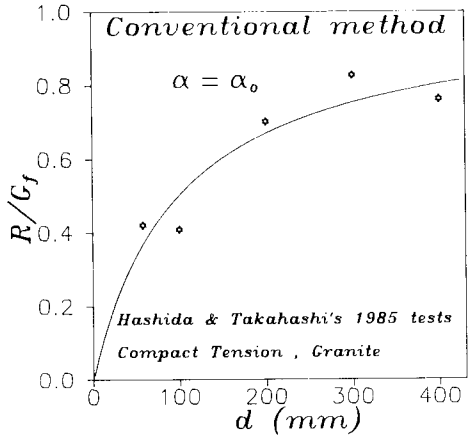

Fig. 8. Plot of fracture energy as a function of size (conventional method, $c = 0$, average $\alpha_0 = 0.544$).

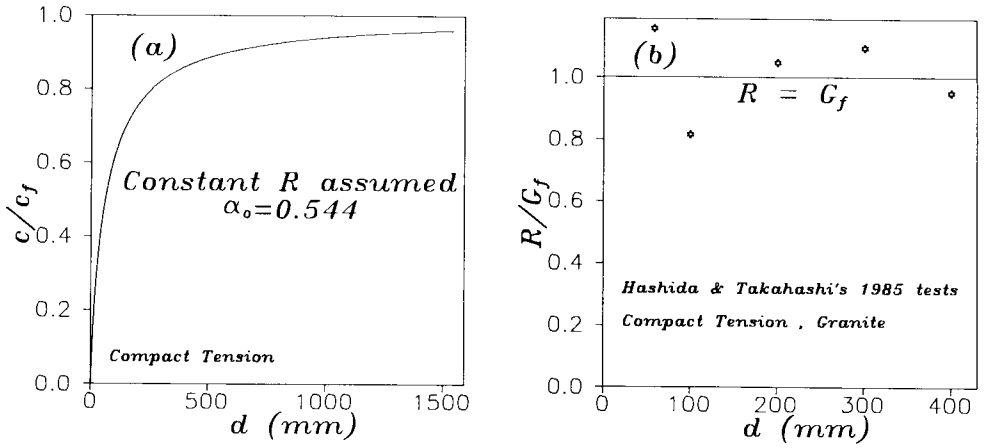

Fig. 9. Dependence of c on size and scatter of CT test results about the line $R = G_f$ (average $\alpha_0 = 0.544$).

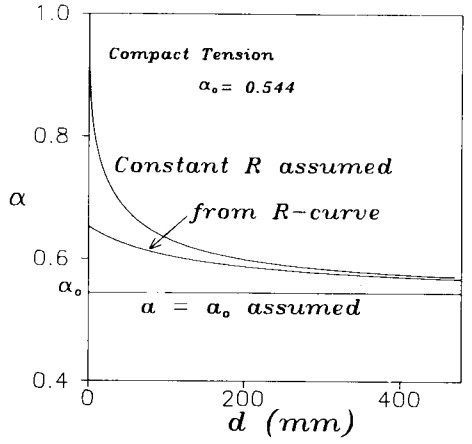

Fig. 10. Plot of relative crack length as a function of size for CT specimens ($\alpha_0 = 0.544$).

As another type of approximation, one can assume that the energy R required for crack growth is approximately constant, $R(c) = G_f$, and that all the nonlinearity of fracture can be attributed to the variation of the fracture process zone length, c. Equating (6) and (9) and considering Bažant's law, (3), one obtains

$$d = \frac{c_f g'(\alpha_0)}{g(\alpha) - g(\alpha_0)}. \tag{36}$$

For any value of α, d can be solved from (36), which then yields the value of c. For $d \to \infty$, for which $\alpha \to \alpha_0$, the limiting value $c \to c_f$ is satisfied. When $d \to 0$, then (36) yields $\alpha \to 1$, i.e., the fracture process zone encompasses the entire specimen.

Figure 9b shows the scatter of the points obtained from the test results around the line $R = G_f$, as obtained for the compact tension tests of Hashida and Takahashi. Figure 9a shows the corresponding dependence of c on size d. In this case, c varies faster than for the case when both R and C are considered variable. Figure 10 shows the relative total crack

length, α, as a function of d for the case where both R and C are considered to vary as well as the simplified cases with either constant a or constant R. We see that these approximations are rather different for very small sizes, but are close to each other as the size becomes large.

10. Conclusions

1. The limiting case of a specimen of infinite size can be used to define not only the fracture energy but also the effective length of the fracture process zone. This definition is independent of both the specimen size and the specimen shape.
2. The dependence of the elastically equivalent crack length on the specimen shape can be expressed by means of the nondimensional energy release rate (obtained according to linear elastic fracture mechanics) and its derivative with respect to the relative crack length.
3. The size effect law proposed by Bažant yields a formula not only for the fracture energy but also for the effective fracture process zone length as a function of the specimen or structure size and shape.
4. The size effect law can be expressed in a form in which the material parameters are the fracture energy and the effective fracture process zone length. Regression analysis of test data on the maximum loads of specimens of various sizes and shapes yields the values of both these parameters. This represents a rather simple method for determining the fracture energy and the effective fracture process zone length, for which only the maximum loads need to be measured.
5. Bažant's brittleness number, which characterizes how close the failure behavior is to linear elastic fracture mechanics or to plastic limit analysis, may be calculated from the effective fracture process zone length and the function expressing the nondimensional energy release rate.
6. The size effect law and the corresponding theoretical results agree with the previously reported fracture tests on rock, as far as the inevitable random scatter of the test results permits it to be discerned. As shown before, they also agree with fracture tests of concrete and aluminum.

Acknowledgement

Partial financial support under AFOSR contract F49620-87-C-0030DEF with Northwestern University, monitored by Dr. Spencer T. Wu, is gratefully acknowledged. In the final phase, partial support was also obtained from NSF Science and Technology Center for Advanced Cement-Based Materials at Northwestern University (NSF grant DMR-8808432).

Appendix. – Previous studies of size effect in rock

The experimental evidence on the effect of specimen size on its strength has been reviewed for a wide range of materials by Sinclair and Chambers [23]. They have noted that the size effect does not follow the linear elastic fracture mechanics. The test results of Costin [24] show that the strength as well as the fracture toughness of oil shale is size dependent.

The same conclusion was made for Nevada tuff by Weisinger, Costin and Lutz [25] on the basis of three-point bending tests. These tests showed that not only the fracture toughness but also the critical value of the J-integral is size dependent.

Kobayashi, Matsuki and Otsuka [26] studied the size effect on Ogino tuff. They reported that while the fracture toughness is almost independent of the specimen thickness and length (perpendicular to the crack plane), it is dependent on the specimen depth (in the direction of the crack). Schmidt and Lutz [27] tested Westerly granite and showed its fracture toughness to be independent of the specimen thickness and dependent on the specimen size. The critical J-integral value they found to be also size dependent, but to a lesser degree.

Zhen and Shi [28] tested seven kinds of rock. To determine the fracture toughness, they used three different methods, one of which was based on the measured values of the maximum loads. In agreement with Bažant's proposition and the test results of Bažant and Pfeiffer [8] for concrete, they concluded that determination of the fracture toughness from the maximum load values for specimens of various sizes gives the most consistent results and shows the least scatter, while at the same time the instrumentation needed is the simplest.

References

1. Z.P. Bažant, in *IUTAM Prager Symposium on Mechanics of Geomaterials: Rocks, Concretes, Soils*, Northwestern University, Evanston, IL., Sept. (1983) 281–316; also *Mechanics of Geomaterials*, Z.P. Bažant (ed.), J. Wiley and Sons, London (1985) 259–303.
2. Z.P. Bažant, Journal of Engineering Mechanics, ASCE 110, No. 4 (1984) 518–535.
3. Z.P. Bažant, in *Fracture Mechanics of Concrete: Structural Application and Numerical Calculation*, Martinus Nijhoff Publishers, Dordrecht (1985) 1–94.
4. Z.P. Bažant, in *Proceedings, U.S. – Japan Seminar on Finite Element Analysis of Reinforced Concrete Structures*, American Society of Civil Engineers, New York (1986) 121–150.
5. Z.P. Bažant, *Applied Mechanics Reviews* 39, No. 5 (1986) 675–705.
6. Z.P. Bažant, J.K. Kim and P.A. Pfeiffer, *Journal of Structural Engineering*, ASCE 112, No. 2 (1986) 289–307.
7. Z.P. Bažant, S. Lee and P.A. Pfeiffer, *Engineering Fracture Mechanics* 26, No. 1 (1987) 45–57.
8. Z.P. Bažant and P.A. Pfeiffer, *ACI Materials Journal* 84, No. 6 (1987) 463–480.
9. Z.P. Bažant, in *SEM/RILEM International Conference on Fracture of Concrete and Rock*, Society for Experimental Mechanics (1987) 390–402; also *Fracture of Concrete and Rock*, S.P. Shah and S.E. Swartz (eds.), Springer Verlag, N.Y. (1989) 229–241.
10. Z.P. Bažant and M.T. Kazemi, "Brittleness and size effect in concrete structures", Engineering Foundation Conference on "Advances in Cement Manufacture and Use", Potosi, Missouri (Aug. 1988).
11. T. Hashida, "Fracture Toughness Evaluation and Hydraulic Fracturing of Rock", Ph.D. thesis, Tohoku University, Sendai, Japan (1984).
12. T. Hashida and H. Takahashi, *Journal of Testing and Evaluation* 13, No. 1 (1985) 77–84.
13. H. Tada, P.C. Paris and G.R. Irwin, *The Stress Analysis of Cracks Handbook*, 2nd ed., Paris Productions, Inc., St. Louis, Mo. (1985).
14. Y. Murakami, *Stress Intensity Factors Handbook*, Pergamon Press (1987).
15. H. Abe, K. Hayashi and T. Hashida, in *SEM/RILEM International Conference on Fracture of Concrete and Rock*, Society for Experimental Mechanics (1987) 572–579; also *Fracture of Concrete and Rock*, S.P. Shah and S.E. Swartz (eds.), Springer Verlag, N.Y. (1989) 354–361.
16. Z.P. Bažant and H. Ohtsubo, *Mechanics Research Communication* 4, No. 5 (1977) 353–366.
17. J.F. Labuz, S.P. Shah and C.H. Dowding, *International Journal of Mechanics, Mineral Science and Geomechanics Abstracts* 24, No. 4 (1987) 235–246.
18. Z.P. Bažant, *Journal of Engineering Mechanics*, ASCE 114, No. 12 (1988) 2013–2034.
19. A. Hillerborg, *Materials and Structures, Research and Testing* (RILEM, Paris) 18, No. 106 (1985) 291–296.
20. A. Carpinteri, *Engineering Fracture Mechanics* 16, No. 4 (1982) 467–481.
21. J.M. Krafft, A.M. Sullivan and R.W. Boyle, in *Crack Propagation Symposium*, Vol. 1, College of Aeronautics, Cranfield, U.K. (1961) 8–28.

22. G.R. Irwin, *ASTM Bulletin* Jan. (1960) 29–40. Also, "Fracture Testing of High Strength Sheet Materials Under Conditions Appropriate for Stress Analysis", Report No. 5486, Naval Research Laboratory, July (1960).
23. G.B. Sinclair and A.E. Chambers, *Engineering Fracture Mechanics* 26, No. 2 (1987) 279–310.
24. L.S. Costin, *Fracture Mechanics Methods for Ceramics, Rocks, and Concrete, ASTM STP 745* (1981) 169–184.
25. R. Weisinger, L.S. Costin and T.J. Lutz, *Experimental Mechanics* 20, No. 2 (1980) 68–72.
26. R. Kobayashi, K. Matsuki and N. Otsuka, *International Journal of Rock Mechanics, Mineral Science & Geomechanics Abstracts* 23, No. 1 (1986) 13–18.
27. R.A. Schmidt and T.J. Lutz, *Fracture Mechanics Applied to Brittle Materials, ASTM STP 678* (1979) 166–182.
28. Y. Zhen and H. Shi, in *SEM/RILEM International Conference on Fracture of Concrete and Rock*, Society for Experimental Mechanics (1987) 170–177.

Résumé. En se reposant sur la loi des effets dimensionnels approximatifs développée par Bažant, on étudie la liasion de dépendance entre la taille de l'éprouvette et l'énergie de rupture, la longueur de la zone de détérioration ainsi que l'étendue de la fissure au départ d'une entaille.

On définit l'énergie de rupture et la longueur effective de la zone où se produit un processus de rupture en se basant sur une extrapolation à une éprouvette de taille infinie, pour laquelle les définitions ne dépendent pas de la forme de l'éprouvette ou de la structure. Ces deux propriétés du matériau sont exprimées en fonction des paramètres de la loi régissant l'effet dimensionnel et d'une relation exprimant de manière non dimensionnelle la vitesse de relaxation de l'énergie.

La loi de Bažant relative à la tension nominale à la rupture est reformulée de manière à ce que les paramètres en soient l'énergie de rupture et la longueur effective (ou son équivalent élastique) de la zone de déterioration.

On donne une méthode de détermination de ces propriétés du matériau à partir de données de, par régressions linéaire et non linéaire. Cette méthode permét d'évaluer ces propriétés sur la seule base du relevé des charges maximum agissant sur des éprouvettes de diverses tailles et, éventuellement, de formes différentes.

On détermine l'évolution de l'énergie de rupture et de la longeur effective de la zone de détérioration en fonction de la dimension de l'éprouvette. Les résultats théoriques sont en accord avec des essais entrepris précédemment sur des roches et sur du béton, et en rendent bien compte, en dépit de l'inévitable dispersion propre aux essais.